Electronic Supplementary Material (ESI) for Nanoscale.

Supporting Information

A 3D mixed ion/electron conducting scaffold by in-situ conversion for long-life lithium metal anodes

Huai Jiang[a], Qingyuan Dong[a], Maohui Bai[a], Furong Qin[a], Maoyi Yi[a], Junquan Lai[a], Bo Hong[a,*], Yanqing Lai[a,b,*]

[a] *School of Metallurgy and Environment, Central South University, Changsha 410083, Hunan, China*

[b] *Engineering Research Centre of Advanced Battery Materials, The Ministry of Education, Changsha 410083, Hunan, China*

***Corresponding authors.**

Email addresses: bop_hong@csu.edu.cn (B. Hong), laiyanqing@csu.edu.cn (Y. Lai)

Tel. and Fax: +86 731 88830649

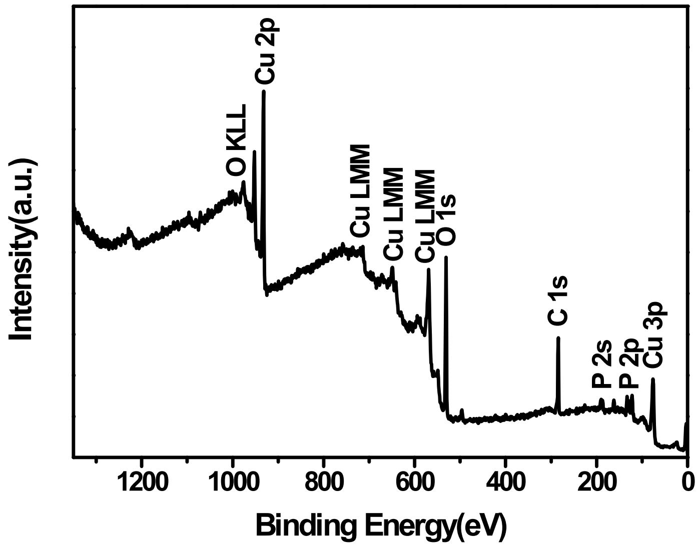

Figure S1. XPS full spectrum of as-synthesized Cu_3P NA@CF.

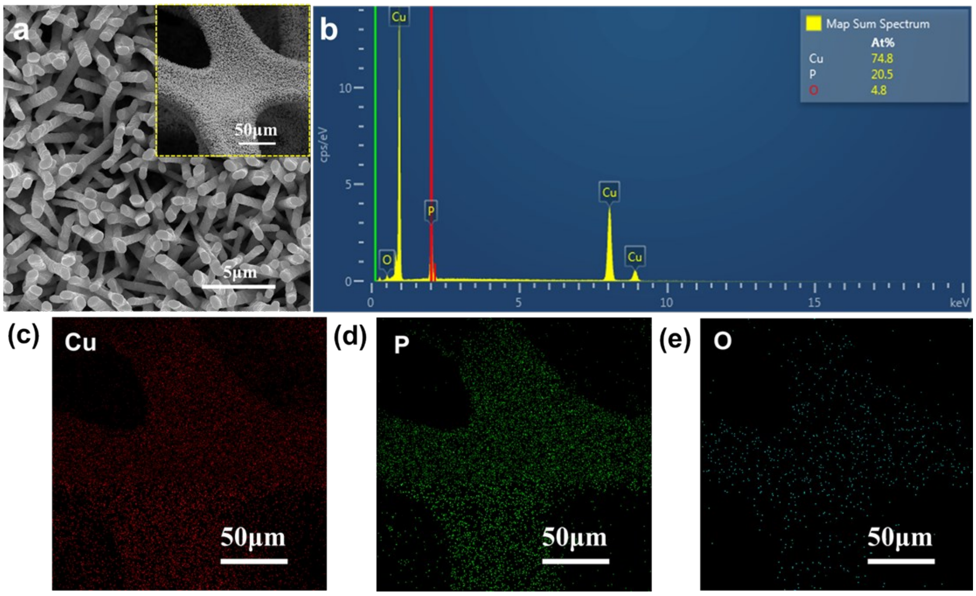

Figure S2. (a) SEM images of the Cu_3P NA@CF under the N/C of 1:1 at 100℃. (b) EDX spectrograms of Cu_3P NA@CF and corresponding elemental mapping images of Cu (c), P (d) and O (e).

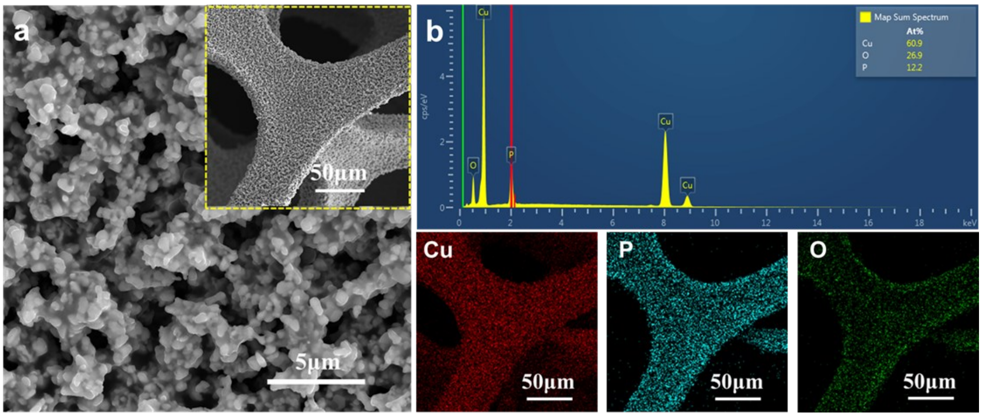

Figure S3. (a) SEM images of the Cu_3P NA@CF under the N/C of 1:2 at 200℃. (b) EDX spectrograms of Cu_3P NA@CF and corresponding elemental mapping images of Cu, P and O.

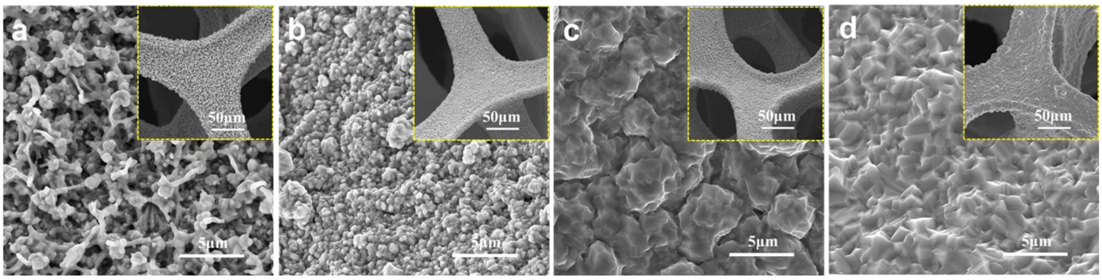

Figure S4. SEM image of the Cu_3P NA@CF with different temperature of phosphating under the N/C of 3:1: (a) 220 ℃; (b) 240 ℃; (c) 260 ℃; (d) 280 ℃.

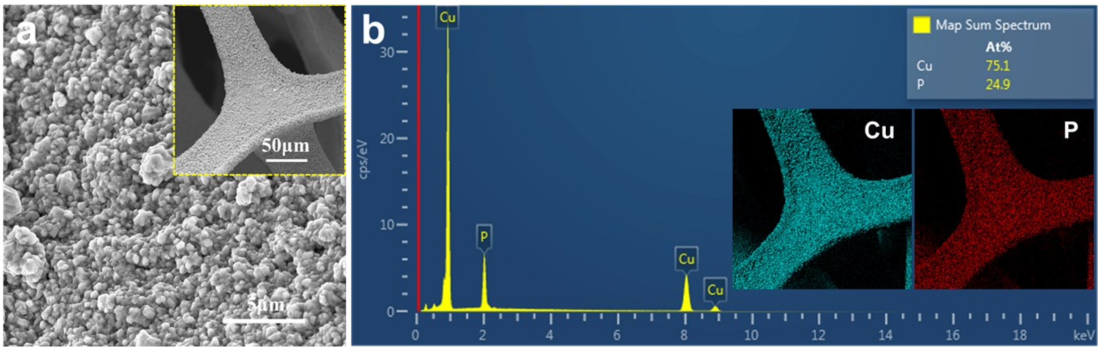

Figure S5. (a) SEM images of the Cu_3P NA@CF under the N/C of 3:1 at 240℃. (b) EDX spectrograms of Cu_3P NA@CF and corresponding elemental mapping images of Cu and P.

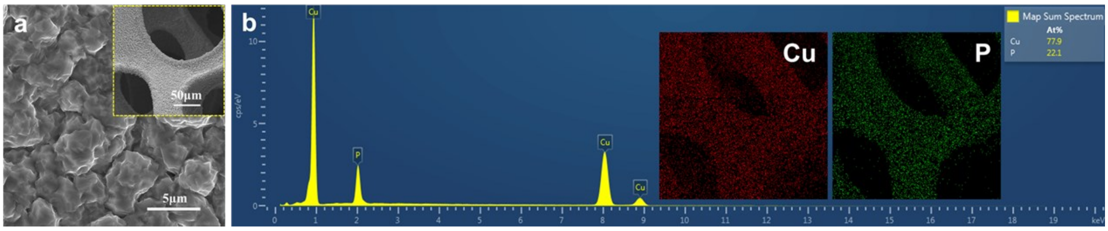

Figure S6. (a) SEM images of the Cu_3P NA@CF under the N/C of 3:1 at 260℃. (b) EDX spectrograms of Cu_3P NA@CF and corresponding elemental mapping images of Cu and P.

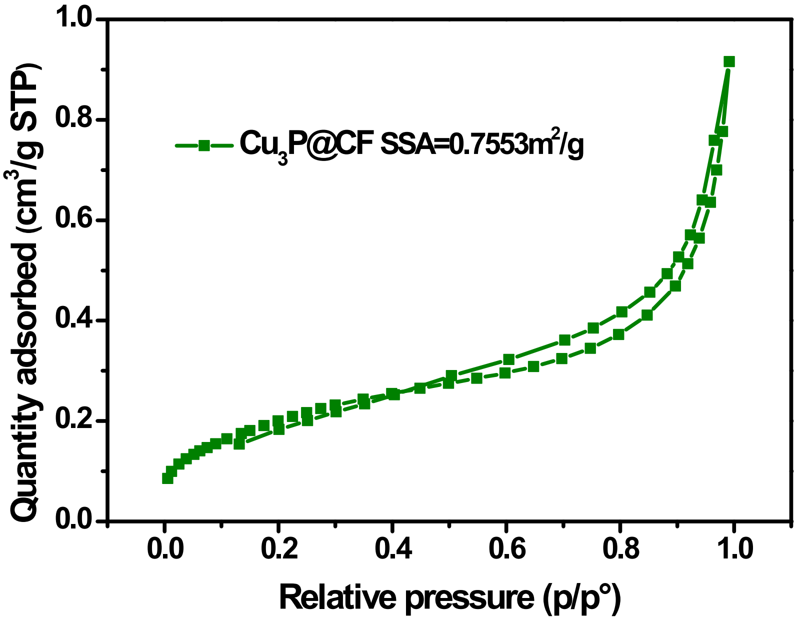

Figure S7. N_2 adsorption–desorption isotherm curve of Cu_3P NA@CF under the N/C of 3:1 at 260°C.

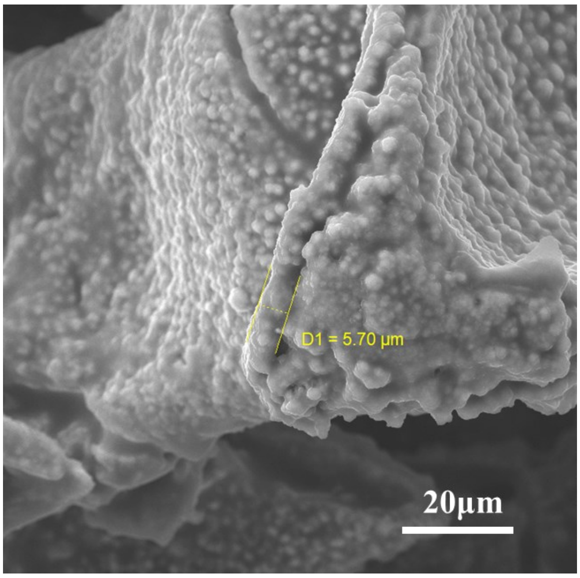

Figure S8. The thickness of Cu_3P coating layer on Cu foam.

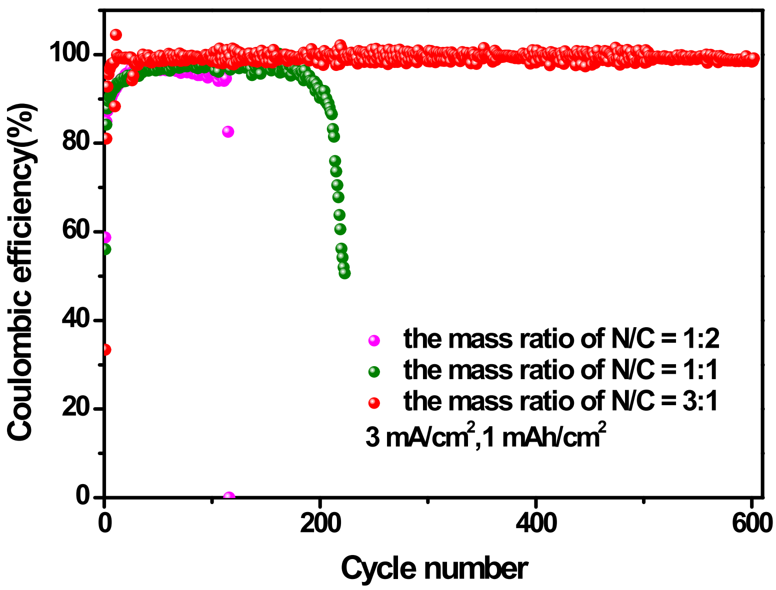

Figure S9. The Coulombic efficiency of Cu_3P NA@CF under the N/C of 1:2, 1:1 and 3:1 at 3 mA cm^{-2} for 1 mAh cm^{-2}.

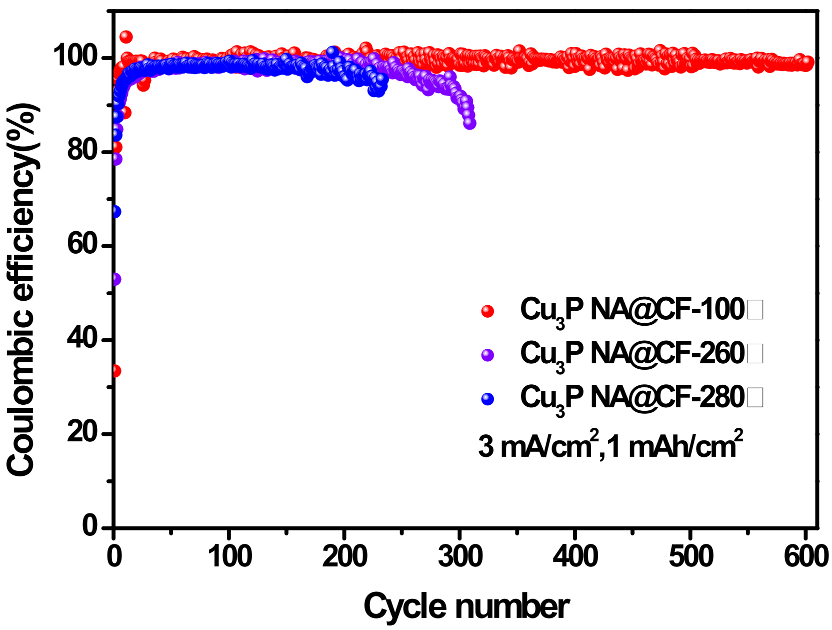

Figure S10. The Coulombic efficiency of the Cu_3P NA@CF with different temperature of phosphating under the N/C of 3:1 at 3 mA cm^{-2} for 1 mAh cm^{-2}.

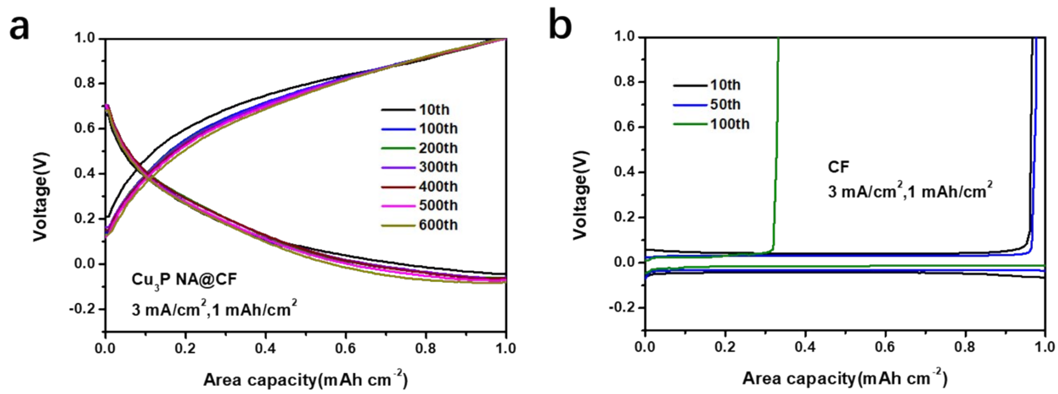

Figure S11. Voltage-capacity profiles for (a) PNF and (b) NF with a current density of 3 mA cm^{-2} and a total capacity of 1 mAh cm^{-2}.

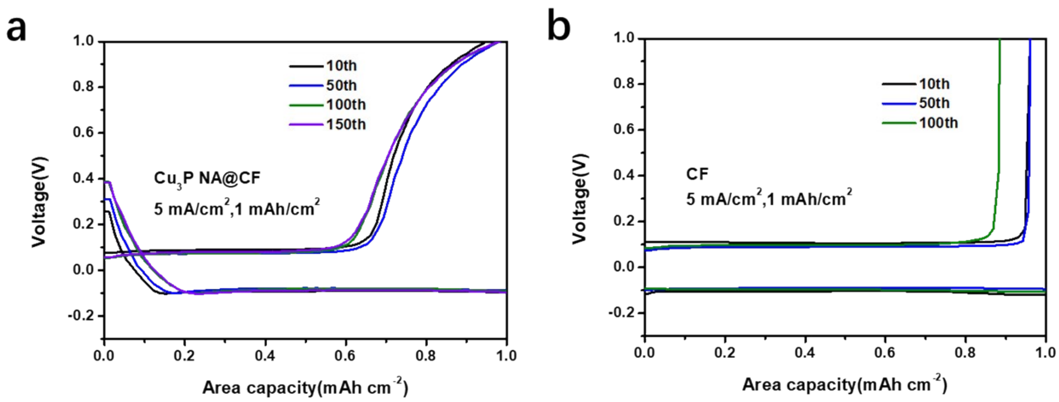

Figure S12. Voltage-capacity profiles for (a) PNF and (b) NF with a current density of 5 mA cm^{-2} and a total capacity of 1 mAh cm^{-2}.

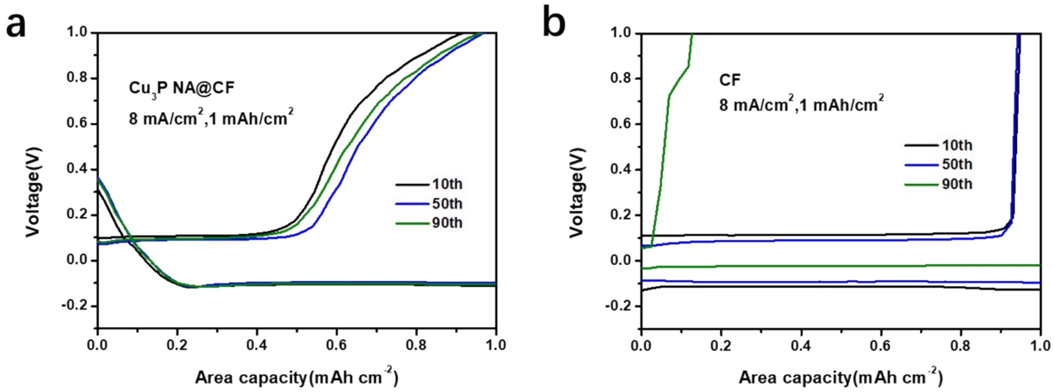

Figure S13. Voltage-capacity profiles for (a) PNF and (b) NF with a current density of 8 mA cm^{-2} and a total capacity of 1 mAh cm^{-2}.

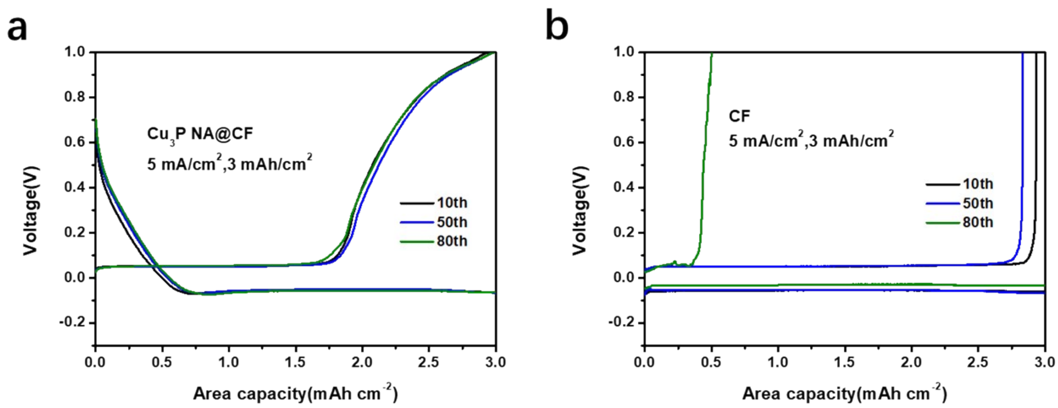

Figure S14. Voltage-capacity profiles for (a) PNF and (b) NF with a current density of 5 mA cm^{-2} and a total capacity of 3 mAh cm^{-2}.

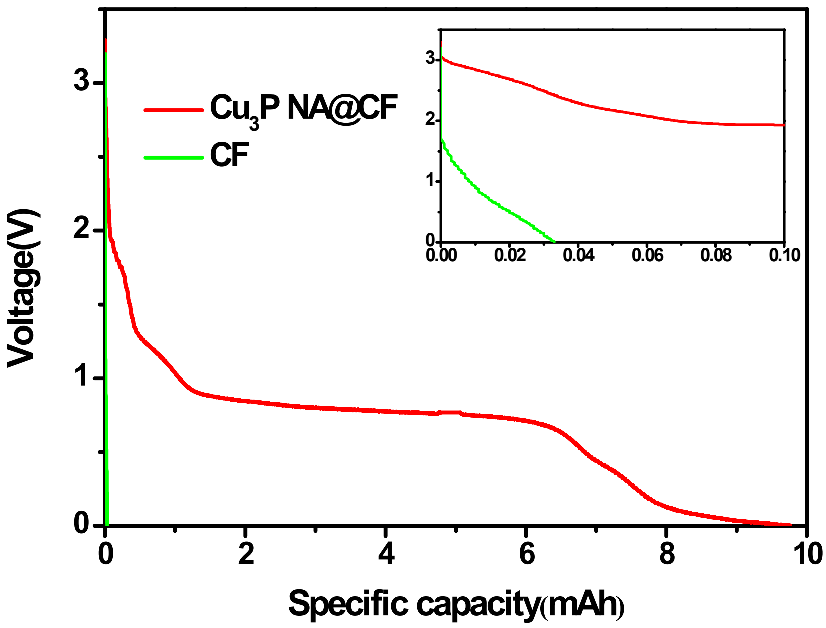

Figure S15. The voltage–capacity curves of Cu_3P NA@CF in the first Li deposition.

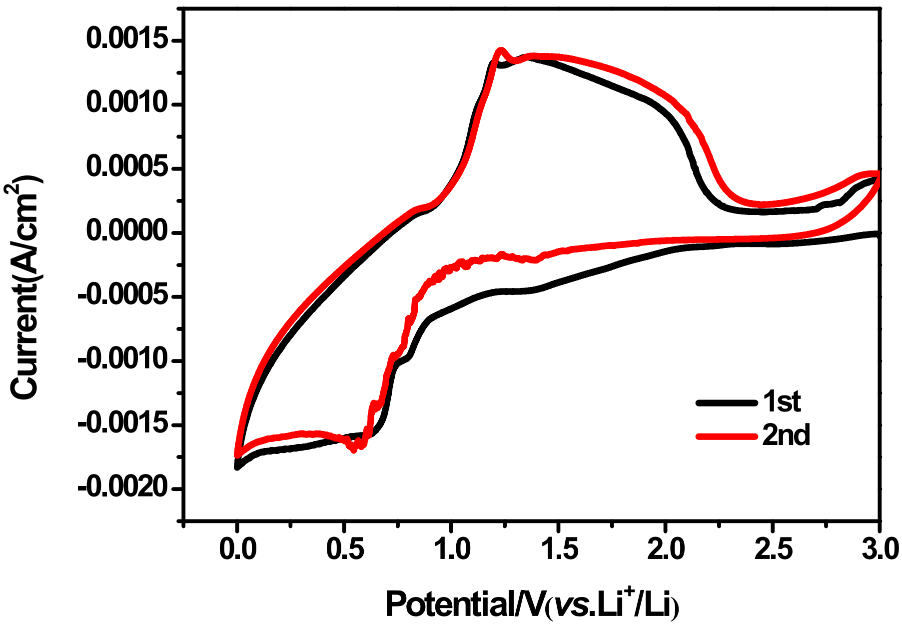

Figure S16. CV curves of the lithiation and delithiation of Cu_3P NA@CF at a sweep speed of 0.1 mV s^{-1} from 0.01 to 3.0 V (vs. Li^+/Li).

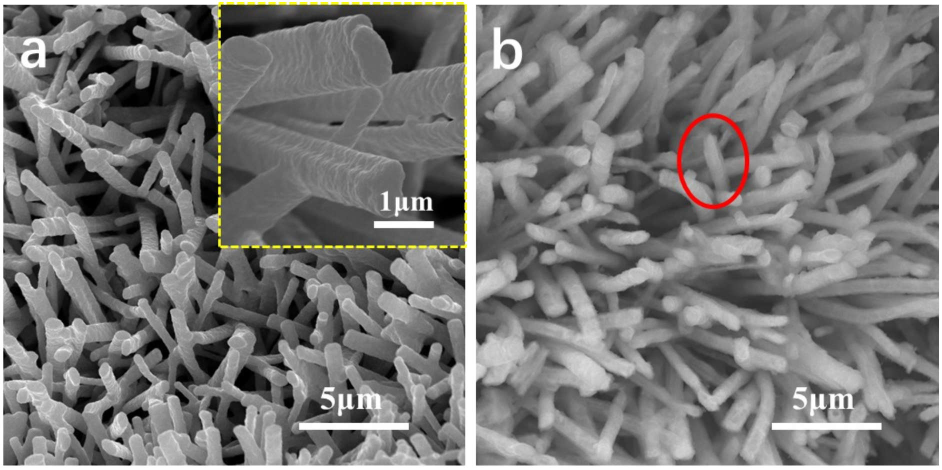

Figure S17. Magnification SEM images of the pristine and 200th stripping on Cu_3P NA@CF at 3 mA cm^{-2} with a total capacity of 1 mAh cm^{-2}.

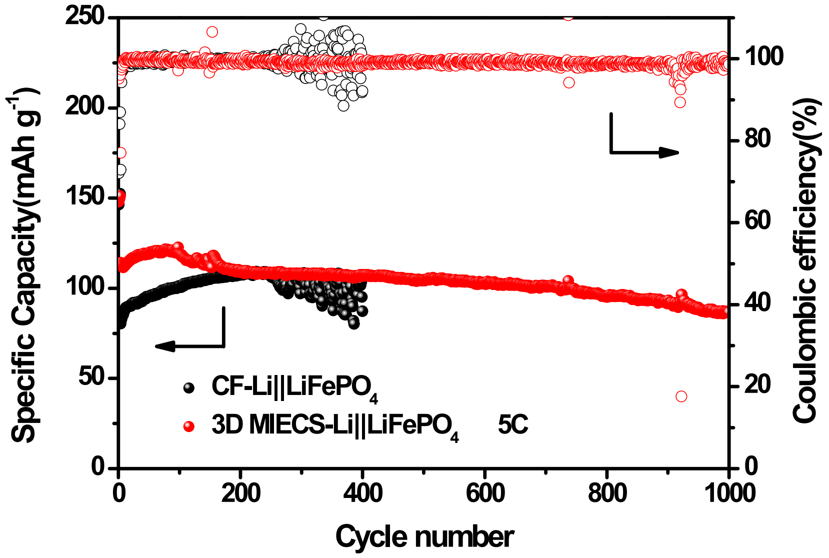

Figure S18. The cycling performance of 3D MIECS-Li||$LiFePO_4$ and CF-Li||$LiFePO_4$ cell at 5 C.

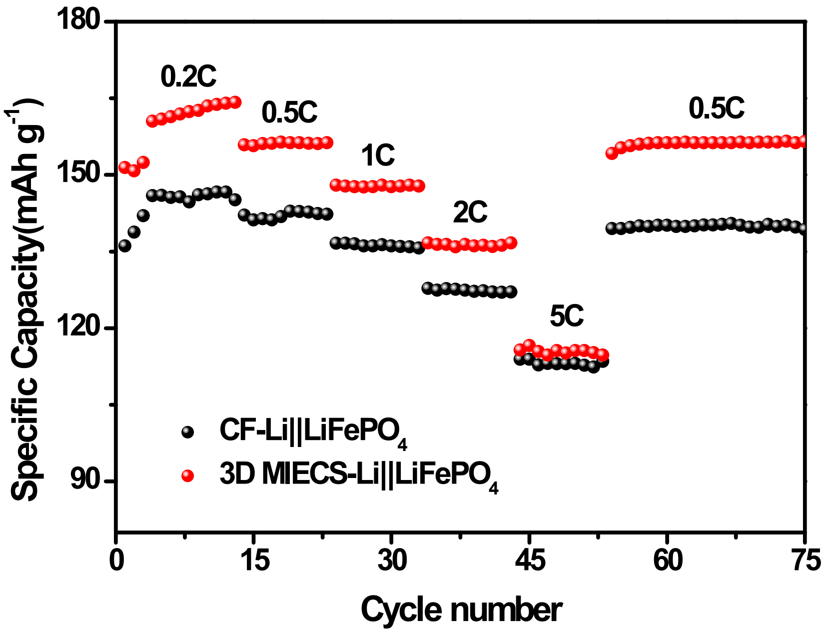

Figure S19. Rate performance between 3D MIECS-Li||$LiFePO_4$ and CF-Li||$LiFePO_4$ cell

Table S1. Comparison of the electrochemical performance of the as-prepared anode with those of

Li metal-based anodes reported recently

Materials	Current density&Capacity	Cycle number	CE (%)	references
Unique 3D nanoporous/macroporous structure Cu current collector	1 mA cm^{-2}, 1 mAh cm^{-2}	200	98	[1]
nitrogen-doped-carbon/ZnO modified Cu foam	3 mA cm^{-2}, 1 mAh cm^{-2}	400	97.6	[2]
Cu_2S nanowires inside the Cu framework	3 mA cm^{-2}, 1 mAh cm^{-2}	100	92	[3]
Lithiophobic-lithiophilic composite architecture	1.5 mA cm^{-2}, 1 mAh cm^{-2}	200	98	[4]
	5 mA cm^{-2}, 3 mAh cm^{-2}	50	96	
3D porous Cu current collector	0.5 mA cm^{-2}, 1 mAh cm^{-2}	70	97	[5]
A self-supported, three-dimensional porous copper film	1 mA cm^{-2}, 1 mAh cm^{-2}	97	120	[6]
Hierarchically Bicontinuous Porous Copper as Advanced 3D Skeleton	3 mA cm^{-2}, 1 mAh cm^{-2}	94	100	[7]
A 3D mixed ion/electron conducting scaffold by in-situ conversion	3 mA cm^{-2}, 1 mAh cm^{-2}	600	99.1	this work
	5 mA cm^{-2}, 1 mAh cm^{-2}	170	98.2	
	5 mA cm^{-2}, 3 mAh cm^{-2}	80	99.35	

References

1 H. Liu, E. Wang, Q. Zhang, Y. Ren, X. Guo, L. Wang, G. Li and H. Yu, *Energy Storage Mater.*, 2019, **17**, 253-259.

2 Y. Zhou, K. Zhao, Y. Han, Z. Sun, H. Zhang, L. Xu, Y. Ma and Y. Chen, *J. Mater. Chem. A*, 2019, **7**, 5712-5718.

3 Z. Huang, C. Zhang, W. Lv, G. Zhou, Y. Zhang, Y. Deng, H. Wu, F. Kang and Q. Yang, *J. Mater. Chem. A*, 2019, **7**, 727-732.

4 Y. Cheng, X. Ke, Y. Chen, X. Huang, Z. Shi and Z. Guo, *Nano Energy*, 2019, **63**, 103854.

5 Q. Li, S. Zhu and Y. Lu, *Adv. Funct. Mater.*, 2017, **27**, 1606422.

6 Y. Shi, Z. Wang, H. Gao, J. Niu, W. Ma, J. Qin, Z. Peng and Z. Zhang, *J. Mater. Chem. A*, 2019, **7**, 1092-1098.

7 X. Ke, Y. Cheng, J. Liu, L. Liu, N. Wang, J. Liu, C. Zhi, Z. Shi and Z. Guo, *ACS Appl. Mater. Inter.*, 2018, **10**, 13552-13561.